HHS Public Access

Author manuscript

Mol Cell. Author manuscript; available in PMC 2016 April 02.

Published in final edited form as:

Mol Cell. 2015 April 2; 58(1): 123–133. doi:10.1016/j.molcel.2015.02.008.

Mitochondrial and nuclear accumulation of the transcription factor ATFS-1 promotes OXPHOS recovery during the UPR^{mt}

Amrita M. Nargund[1], **Christopher J. Fiorese**[1,2], **Mark W. Pellegrino**[1], **Pan Deng**[1,2], and **Cole M. Haynes**[1,2,*]

[1]Cell Biology Program, Memorial Sloan Kettering Cancer Center, New York, New York 10065, USA

[2]BCMB Allied Program, Weill Cornell Medical College, 1300 York Avenue, New York, New York 10065, USA

Summary

Mitochondrial diseases and aging are associated with defects in the oxidative phosphorylation machinery (OXPHOS), which are the only complexes composed of proteins encoded by separate genomes. To better understand genome coordination and OXPHOS recovery during mitochondrial dysfunction, we examined ATFS-1, a transcription factor that regulates mitochondria-to-nuclear communication during the mitochondrial UPR, via ChIP-sequencing. Surprisingly, in addition to regulating mitochondrial chaperone, OXPHOS complex assembly factor, and glycolysis genes, ATFS-1 bound directly to OXPHOS gene promoters in both the nuclear and mitochondrial genomes. Interestingly, *atfs-1* was required to limit the accumulation of OXPHOS transcripts during mitochondrial stress, which required accumulation of ATFS-1 in the nucleus and mitochondria. Because balanced ATFS-1 accumulation promoted OXPHOS complex assembly and function, our data suggest that ATFS-1 stimulates respiratory recovery by fine-tuning OXPHOS expression to match the capacity of the suboptimal protein-folding environment in stressed mitochondria, while simultaneously increasing proteostasis capacity.

Introduction

Mitochondria generate ATP via chemical reactions mediated by the tricarboxylic acid (TCA) cycle and OXPHOS. The TCA cycle requires eight mitochondrial matrix-localized enzymes while OXPHOS requires the four respiratory chain complexes and the ATP synthase. The OXPHOS complexes are comprised of over 70 proteins that assemble into individual complexes on the mitochondrial inner membrane with the assistance of molecular chaperones and complex-specific assembly factors (Mimaki et al., 2012). Nuclear genes

To whom correspondence should be addressed. haynesc@mskcc.org.

Accession Numbers: The NCBI Gene Expression Omnibus accession number fro the ChIP-seq data reported is GSE63803.

encode most subunits, but 13 are encoded by the mitochondrial genome (mtDNA) (Pagliarini et al., 2008) (12 in *C. elegans* (Bratic et al., 2010)). Therefore, expression from each genome must be coordinated to promote proper stoichiometry, efficient assembly and prevent the accumulation of deleterious orphaned subunits (Nolden et al., 2005; Rugarli and Langer, 2012).

Mitochondrial dysfunction occurs during aging as well as in a number of diseases, however the mechanisms a cell employs to stabilize defective mitochondria and regenerate functional OXPHOS complexes under such conditions are unclear (Rugarli and Langer, 2012; Vafai and Mootha, 2012). The UPR^{mt} is a mitochondrial-specific stress response mediated by the bZip transcription factor ATFS-1, which is normally efficiently imported into mitochondria and degraded. However, during mitochondrial dysfunction, a percentage of ATFS-1 fails to be imported and accumulates in the cytosol. Because ATFS-1 has a nuclear localization sequence (NLS), it traffics to the nucleus and mediates the induction of protective genes including mitochondrial chaperones and proteases, antioxidant machinery as well as components of the glycolysis pathway (Nargund et al., 2012). These findings suggest that the UPR^{mt} serves to stabilize the mitochondrial protein-folding environment and up-regulate a separate source of ATP production to promote survival and ultimately recover mitochondrial function (Haynes et al., 2013; Houtkooper et al., 2013; Nargund et al., 2012). However, the cellular processes affected by ATFS-1 and UPR^{mt} activation have yet to be fully resolved.

Transcription of nuclear-encoded OXPHOS genes is regulated by multiple transcription factors in mammals including NRF-1, NRF-2, PPARα, the estrogen-related receptors and the transcriptional co-activator PGC-1 (Scarpulla et al., 2012; Schreiber et al., 2004; Wu et al., 1999). The remaining OXPHOS subunits are transcribed from mtDNA via a process that has been extensively characterized in mammalian systems and requires three nuclear-encoded components; the mitochondrial RNA polymerase (POLRMT), a transcription initiation factor mtTFB2/TFB2M, and TFAM which functions as a transcriptional activator as well as a mtDNA packaging protein (Bestwick and Shadel, 2013; Falkenberg et al., 2007).

Once transcribed, the OXPHOS subunits are translated by cytosolic or mitochondrial ribosomes and trafficked to the mitochondrial inner membrane where they assemble into stoichiometric complexes, which presents considerable challenges. For example, the individual OXPHOS components are highly expressed and require multiple assembly factors and chaperones to efficiently complete the assembly process. Orphaned subunits that fail to incorporate into functional complexes can be degraded by either the i-AAA or m-AAA proteases located in the mitochondrial inner membrane facing the intermembrane space and matrix, respectively (Leonhard et al., 2000; Rugarli and Langer, 2012). Interestingly, subunits of both protease complexes are induced by ATFS-1 during stress (Nargund et al., 2012), suggesting complex assembly is especially challenging during mitochondrial dysfunction.

To complement our previous mRNA profiling experiments, we performed chromatin immunoprecipitation coupled with DNA sequencing (ChIP-seq) to determine where in the

genome ATFS-1 bound during mitochondrial stress. In addition to mitochondrial protective and glycolysis genes, ATFS-1 interacted with the promoters of TCA cycle and OXPHOS genes suggesting that ATFS-1 regulates multiple metabolic pathways. Interestingly, in addition to interacting with nuclear DNA, ATFS-1 also bound mtDNA. Surprisingly, we found that *atfs-1* acts as a negative regulator of TCA cycle and OXPHOS transcript accumulation. And, balanced mitochondrial and nuclear accumulation of ATFS-1 is essential for coordinated OXPHOS gene expression, efficient OXPHOS complex assembly, respiration, and development during mitochondrial dysfunction. Thus, in addition to increasing mitochondrial protein folding and complex assembly capacity, our data suggest that ATFS-1 stimulates OXPHOS recovery by fine-tuning OXPHOS biogenesis rates to match the capacity of the suboptimal mitochondrial protein-folding environment.

Results

ATFS-1 interacts with the promoters of mitochondrial protective genes induced during mitochondrial stress

Our previous gene expression profiling studies identified 381 genes that were induced during mitochondrial stress dependent on *atfs-1* (Nargund et al., 2012). To determine where in the genome ATFS-1 bound and potentially which genes were regulated by ATFS-1, we performed ChIP-seq. Mitochondrial stress was induced by RNAi knockdown of *spg-7*, a component of the m-AAA protease required for mitochondrial ribosome biogenesis and OXPHOS component quality control (Leonhard et al., 2000; Rugarli and Langer, 2012). Of the 381 genes transcriptionally induced by ATFS-1 during mitochondrial stress (Nargund et al., 2012), ATFS-1 interacted with 70 of the corresponding gene promoters (Figure 1A, Tables S1-S2), which included genes such as the mitochondrial chaperones *mthsp-70* (*hsp-6*) (Figure 1B), *dnj-10* (Figure S1A) and *hsp-60* (Figure 2), the i-AAA protease *ymel-1* (Figure 1C), and the glycolysis component *gpd-2* (Figure 1D). ATFS-1 was also enriched at the promoters of many other genes required for mitochondrial function including the mitochondrial fission component *drp-1* (Figure S1B) and components of the mitochondrial protein import machinery including *timm-17* and *timm-23* (Figures S1C-D). Of note, ATFS-1 did not bind or activate the promoter of the endoplasmic reticulum (ER) localized chaperone *hsp-4* (Figures 1E and 1M) consistent with ATFS-1 regulating a mitochondrial-protective response (Nargund et al., 2012).

To validate ATFS-1 binding, ChIP followed by qPCR was performed to determine if ATFS-1 preferentially bound these promoters specifically during stress (Figures 1F-I). Consistent with ATFS-1 accumulating in the nucleus during mitochondrial stress (Nargund et al., 2012), ATFS-1 was enriched at the *mthsp-70*, *ymel-1*, and *gpd-2* promoters only during mitochondrial dysfunction which coincided with increased transcripts, (Figures 1J-L), suggesting ATFS-1 directly regulates expression of these genes.

Alternatively, 311 genes were induced during mitochondria stress but were not bound by ATFS-1 (Table S1-S2), suggesting indirect regulation. For example, over twenty genes involved in reactive oxygen species (ROS) detoxification were induced in an *atfs-1*-dependent manner (Nargund et al., 2012), but ATFS-1 did not interact with any of the corresponding promoters (Table S1). However, during mitochondrial stress ATFS-1 did

bind and activate the promoter of the gene encoding SKN-1, the transcription factor previously shown to directly regulate induction of many ROS-detoxifying genes (Figure S1E and (Oliveira et al., 2009)).

ATFS-1 binds a UPR^{mt}E to induce mitochondrial protective gene transcription

To identify promoter regulatory sequences, or UPR^{mt} elements (UPR^{mt}Es), we performed motif analysis of the genomic regions to which ATFS-1 bound in the promoters of mitochondrial protective genes transcriptionally induced during mitochondrial stress. Four potential elements were identified, but we focused on a 14 base pair sequence (Figures 2A and S2A-D) that was the most enriched, suggesting a role for this sequence in ATFS-1-dependent gene regulation.

To examine the function of the putative UPR^{mt}E, transgenic worms expressing GFP via the *hsp-60* promoter were employed (Nargund et al., 2012). As expected, ATFS-1 interacted with the multi-copy transgenic promoter during mitochondrial stress as determined by ChIP-seq and ChIP-qPCR (Figures 2B-C). And, as previously documented, the wild-type promoter was activated, as indicated by *hsp-60* mRNA induction and increased GFP fluorescence, when the worms were raised on *spg-7*(RNAi) (Figures 2D-E). However, deletion of one of the three UPR^{mt}Es in the *hsp-60* promoter impaired $hsp\text{-}60_{pr.}$:*gfp* induction during stress (Figure 2E), similar to *atfs-1*-deletion. Of note, deletion of one UPR^{mt}E impaired, but did not completely block, $hsp\text{-}60_{pr.}$:*gfp* induction as longer exposures to mitochondrial stress resulted in modest $hsp\text{-}60_{pr.}$:*gfp* induction (Figures 2E, S2E), consistent with all three UPR^{mt}Es contributing to *hsp-60* regulation. Combined, these data suggest that ATFS-1 binds to this 14 base pair sequence to regulate mitochondrial protective gene induction during mitochondrial stress. UPR^{mt}Es were not present in the promoter of *hsp-4*, consistent with the ER chaperone not being induced during mitochondrial stress (Figure 1M).

ATFS-1 interacts with the promoters of genes in multiple metabolic pathways

In addition to those genes identified previously, ChIP-seq indicated that ATFS-1 bound to the promoters of 851 additional genes (Figure 1A), suggesting that ATFS-1 may regulate a much broader set of transcripts than previously appreciated (Nargund et al., 2012). The five most enriched pathways identified by Gene Enrichment and Functional Annotation tool provided by the Database of Annotation, Visualization, and Integrated discovery (DAVID) (Dennis et al., 2003), were glycolysis/gluconeogenesis, ribosome, oxidative phosphorylation, the tricarboxylic acid (TCA) cycle and autophagy (Figure 3A, Table S3) suggesting ATFS-1 modulates multiple metabolic pathways.

We next sought to determine if *atfs-1* regulates transcription or transcript accumulation of the genes enriched in our ChIP-seq data. *atfs-1*-deletion did not affect the accumulation of the ribosomal or autophagy transcripts (Figures S3C-D). And as expected, *atfs-1* was required for the induced expression of multiple glycolysis genes as well as lactate dehydrogenase during mitochondrial stress (Figures 3B and 3D). TCA cycle mRNAs were also induced during mitochondrial stress. But interestingly, they were further induced in

atfs-1-deletion worms suggesting ATFS-1 negatively regulates TCA cycle transcript accumulation (Figure 3E).

Each of the five OXPHOS complexes consists of multiple subunits and all but the succinate dehydrogenase complex are composed of both nuclear and mtDNA-encoded components. ChIP-seq indicated that ATFS-1 bound to several promoters of genes that encode components of each complex including *nuo-4* (NADH ubiquinone oxidoreductase, I), *sdha-1* (succinate dehydrogenase, II), *ucr-2.1* and *cyc-2*.1 (cytochrome c reductase, III), *cco-1* (cytochrome c oxidase, IV) and *atp-3* (ATP synthase, V) (Figures 4A-F, Table S1). Similar to the TCA cycle mRNAs, these OXPHOS transcripts were also increased in *atfs-1*-deletion worms during mitochondrial stress (Figures 4G-L), indicating *atfs-1* also negatively regulates OXPHOS transcript accumulation.

Interestingly, ATFS-1 did not interact with many OXPHOS gene promoters during mitochondrial stress including *nuo-2*, *nuo-6*, *sdhb-1*, *isp-1*, *cyc-2*.2, *cco-2*, *atp-4*, and *atp-5* (Table S1). However, these transcripts were also further increased in *atfs-1*-deletion worms (Figures S4A-H) indicating that *atfs-1* is also a negative regulator of these transcripts although the mechanism is likely indirect (see Discussion). We examined the promoters of TCA cycle and OXPHOS genes bound by ATFS-1 for potential regulatory sequences but were unable to identify any consensus elements consistent with binding by a bZip transcription factor (Figure S4I) (Buske et al., 2010).

spg-7(RNAi) was utilized throughout these studies to induce mitochondrial stress, however similar results were obtained using the *clk-1(qm30)* allele; a deletion that impairs ubiquinone biogenesis and previously demonstrated to activate the UPR^{mt}, albeit to a lesser degree than *spg-7*(RNAi) (Baker et al., 2012; Nargund et al., 2012). In *clk-1(qm30)* worms, *atfs-1*(RNAi) decreased *hsp-60* mRNA (Figure S4J) while causing an increase in nuclear-encoded OXPHOS transcripts (Figure S4K-L) indicating that ATFS-1 negatively regulates OXPHOS transcript levels during multiple forms of mitochondrial stress.

ATFS-1 associates with mtDNA during mitochondrial stress

ChIP-seq also revealed that during mitochondrial stress, ATFS-1 bound to the non-coding region of mtDNA (Figure 5A), suggesting a role for ATFS-1 in mtDNA regulation. Consistent with multiple copies of mtDNA per cell, the number of ChIP-seq reads in mtDNA was greater than all nuclear interactions (Figures 5A and 1B-D). Because mtDNA sequences also exist in the *C. elegans* nuclear genome, we eliminated those sequences acquired by ATFS-1 ChIP-seq that mapped to multiple regions of the genome. Even with the increased stringency, ATFS-1 binding was still significantly enriched in the mtDNA non-coding region (Figure S5A).

ATFS-1 binding to mtDNA was specifically enriched during mitochondrial stress (Figure 5B), which required ATFS-1-specific antibodies (Figure 5B) and was reduced in *atfs-1(tm4525)* worms (Figure S5B). While the regulatory segments of *C. elegans* mtDNA have not been extensively characterized, ATFS-1 binding was most enriched in an A-T-rich segment lacking protein or RNA coding genes (Figure 5A) suggested to be the regulatory region or D-loop (Bratic et al., 2010). Interestingly, this segment contained a UPR^{mt}E in the

region where ATFS-1 binding was most enriched (Figures 5A and 5C). Similar to the ChIP experiments, an electrophoretic mobility shift assay (EMSA) indicated that recombinant ATFS-1 bound to double stranded oligonucleotides identical to the *C. elegans* mtDNA non-coding region that contained the UPR^{mt}E (Figure 5D and Table S7). Importantly, ATFS-1 binding was reduced when the UPR^{mt}E was scrambled (Figure 5D), suggesting that ATFS-1 binds the mtDNA UPR^{mt}E directly.

During mitochondrial stress, ATFS-1 import is impaired allowing a percentage of ATFS-1 to traffic to the nucleus (Nargund et al., 2012). However, ChIP-seq (Figure 5A) and ChIP-qPCR (Figures 5B and S5B) indicated that ATFS-1 also accumulates in mitochondria during stress. Consistent with this data, subcellular fractionation indicated that multiple isoforms or fragments of ATFS-1 accumulated in mitochondria during stress (Figure 5E), similar to our previous report (Nargund et al., 2012). The mechanism(s) that contribute to the increased accumulation of ATFS-1 within mitochondria during stress are not entirely clear. However, ATFS-1 interacted with the *atfs-1* promoter and *atfs-1* transcription was significantly induced (Figures S5C-E) consistent with an increase in ATFS-1 expression during mitochondrial stress (Figure 5E). Two splice variants of *atfs-1* have been identified that encode proteins of 472 and 488 amino acids but with the same MTS (Figure S5F). Interestingly, only the shorter isoform was transcriptionally induced during mitochondrial stress (Figures S5G-H) suggesting this variant lacking a 48 base pair intron that encodes a 16 amino acid sequence may preferentially interact with mtDNA. Unfortunately, our ATFS-1 antibodies do not distinguish between the splice variants. Thus, we cannot exclude potential effects of altered ATFS-1 protein processing within mitochondria contributing to its stabilization.

atfs-1 represses the accumulation of mtDNA-encoded transcripts during the UPR^{mt}

We next sought to determine if mitochondrial-localized ATFS-1 regulates mtDNA during mitochondrial dysfunction. mtDNA levels were not significantly altered during mitochondrial stress in wild-type or in *atfs-1(tm4525)* worms (Figure 5F), suggesting that ATFS-1 does not regulate mtDNA replication or turnover.

To determine if *atfs-1* affects mtDNA-encoded transcripts, the steady state levels of multiple mtDNA-encoded mRNAs were examined in wild-type and *atfs-1(tm4525)* worms. Consistent with a compensatory response to regenerate OXPHOS complexes during mitochondrial dysfunction, mtDNA-encoded transcripts were modestly induced during stress (Figures 5G-J and S5I-K). However, in *atfs-1*-deletion worms, the mtDNA-encoded transcripts were further increased (Figures 5G-J and S5I-K) suggesting that *atfs-1* negatively regulates the accumulation of mtDNA-encoded OXPHOS transcripts similar to the nuclear-encoded OXPHOS transcripts. All mtDNA-encoded transcripts examined were further increased in *atfs-1*-deletion worms consistent with increased transcription of a polycistronic transcript, however we cannot exclude the effects of *atfs-1* on mRNA turnover. mtDNA-encoded transcripts were also increased when *clk-1(qm30)* worms were raised on *atfs-1*(RNAi) (Figures S5L-M). In sum, these results indicate that ATFS-1 accumulates within mitochondria and that *atfs-1* is a negative regulator of mtDNA-encoded OXPHOS transcript accumulation.

Mitochondrial localization of ATFS-1 is required to limit the accumulation of mtDNA-encoded mRNAs during stress

Despite the accumulation of ATFS-1 within mitochondria and the interaction of ATFS-1 with mtDNA, it remained possible that an ATFS-1-induced nuclear-encoded protein mediated mtDNA-encoded transcript accumulation. We first considered the three nuclear-encoded genes required for mtDNA transcription (Bestwick and Shadel, 2013; Falkenberg et al., 2007). The mitochondrial RNA polymerase *rpom-1* was induced in an *atfs-1*-dependent manner during stress while the TFAM (*hmg-5*) and TFB2M (*tfbm-1*) encoding genes were either not affected or not increased (Figures S5N-P), indicating that transcriptional induction of these genes in the absence of *atfs-1* does not contribute to the increased mtDNA-encoded transcripts.

We next sought to determine if mitochondrial localization of ATFS-1 is required to regulate mtDNA-encoded transcript accumulation during stress. We utilized previously described *atfs-1* deletion strains that express transgenic wild-type ATFS-1 or ATFS-1 lacking the MTS (ATFS-$1^{\Delta 1\text{-}32.myc}$) (Figure 5K) (Nargund et al., 2012). Of note, while ATFS-$1^{\Delta 1\text{-}32.myc}$ cannot be imported into mitochondria it does accumulate within nuclei (Nargund et al., 2012) and induced nuclear transcription similar to that observed in wild-type worms during stress (Figure 5L).

As expected, mitochondrial stress caused a modest induction of the mtDNA-encoded complex III gene *ctb-1*, which was further increased in *atfs-1(tm4525)* worms (Figure 5J, columns 1-3). And, transgenic expression of wild-type ATFS-1 limited the accumulation of the mtDNA-encoded transcript (Figure 5J, column 4), similar to that observed in wild-type worms. Interestingly, expression of ATFS-$1^{\Delta 1\text{-}32.myc}$, which cannot be imported into mitochondria, failed to limit the accumulation mtDNA-encoded mRNAs (Figure 5J, column 5) indicating that mitochondrial localization of ATFS-1 is required. Because ATFS-$1^{\Delta 1\text{-}32.myc}$ activates nuclear transcription (Figure 5L), a downstream nuclear-encoded target of ATFS-1 is not likely required for the negative regulation of mtDNA-encoded transcripts. Additionally, transgenic expression of ATFS-$1^{\Delta NLS}$, which has attenuated nuclear activity (Figure 5J, column 6) but still traffics to mitochondria (Nargund et al., 2012), also limited the accumulation of the mtDNA-encoded transcripts in *atfs-1*-deletion worms further demonstrating that the mitochondrial activity of ATFS-1 can be separated from its nuclear function. Thus, in addition to inducing transcription of genes that promote mitochondrial proteostasis, ATFS-1 also limits the accumulation of nuclear and mtDNA-encoded OXPHOS transcripts during stress.

ATFS-1 promotes OXPHOS complex assembly during mitochondrial dysfunction

In addition to mitochondrial molecular chaperones and proteases, which promote OXPHOS complex assembly (Mimaki et al., 2012 Rugarli and Langer, 2012), ATFS-1 also bound the promoters of OXPHOS complex assembly factors and iron-sulfur biogenesis components which are required for OXPHOS complex biogenesis (Ghezzi and Zeviani, 2012) (Table S1). Specifically, ATFS-1 bound the promoters of *nuaf-1* and *Y17G9B.5* (*ECSIT*), two NADH ubiquinone oxidoreductase assembly factors, and *lpd-8* (NFU1), a Fe-S cluster biogenesis component (Figures 6A-C). These genes were induced during mitochondrial

stress in an *atfs-1*-dependent manner (Figures 6D-F) suggesting a role for ATFS-1 in OXPHOS complex assembly.

We next examined the abundance of individual OXPHOS proteins as well as OXPHOS complexes in wild-type and *atfs-1*-deletion worms. We were unable to detect altered steady-state levels of a mtDNA-encoded protein during mitochondrial stress (Figure 6G) consistent with post-transcriptional regulation of OXPHOS components during mitochondrial dysfunction (Mick et al., 2011). However, the accumulation of two nuclear encoded OXPHOS proteins was increased during mitochondrial stress. Consistent with *atfs-1* limiting OXPHOS mRNA accumulation (Figures 4 and 5), *atfs-1(tm4525)* worms expressed higher levels of NDUFS3 (complex I) and ATP5A (complex V) when raised on *spg-7*(RNAi) (Figure 6H, top three panels). Despite the increased nuclear and mtDNA-encoded OXPHOS mRNAs and nuclear-encoded protein components in *atfs-1*-deletion worms, assembly of complexes I and V was reduced, as determined by blue-native PAGE gels (Figure 6H, lower two panels). Consistent with reduced respiratory chain and ATP synthase assembly, *atfs-1*-deletion worms consumed less oxygen during mitochondrial stress (Figure 6I), suggesting ATFS-1 promotes OXPHOS.

Mitochondrial and nuclear accumulation of ATFS-1 promotes respiration and development during mitochondrial dysfunction

A challenge to determining the biological significance of *atfs-1*-dependent OXPHOS gene regulation is the difficulty in separating this activity of ATFS-1 from its role in promoting proteostasis by upregulating transcription of mitochondrial chaperone and assembly factors (Figures 1 and 6D-F). We utilized worms expressing ATFS-1$^{\Delta 1\text{-}32myc}$, which regulates nuclear transcription similar to wild-type ATFS-1 during mitochondrial stress (Figure 7A), but does not traffic to mitochondria and cannot regulate mtDNA-encoded transcripts (Figure 5J). Interestingly, worms expressing ATFS-1$^{\Delta 1\text{-}32myc}$ had less assembled complexes than worms expressing wild-type ATFS-1 (Figure 7B) and consumed less oxygen (Figure 7C) during mitochondrial stress, demonstrating the importance of mitochondrial localized ATFS-1. As expected, *atfs-1*-deletion worms expressing ATFS-1$^{\Delta NLS}$ displayed defects in OXPHOS complex assembly (Figure 7D) and had reduced oxygen consumption (Figure 7E), consistent with reduced nuclear activity (Figure 5L). Combined, these results indicate that like nuclear-localized ATFS-1, mitochondrial-localized ATFS-1 promotes OXPHOS complex assembly and function during mitochondrial dysfunction.

Furthermore, transgenic worms expressing ATFS-1$^{\Delta 1\text{-}32myc}$ developed slower than transgenic worms expressing wild-type ATFS-1 (Figure 7F). This developmental defect was partially rescued when ATFS-1$^{\Delta 1\text{-}32myc}$ was expressed in *atfs-1* wild-type worms in which endogenous ATFS-1 accumulates in mitochondria (Figure 7G). Because ATFS-1$^{\Delta 1\text{-}32myc}$ expressing worms activate the nuclear response, but fail to limit mtDNA encoded transcripts (Figure 5J), these results indicate that ATFS-1's role in limiting mtDNA-encoded OXPHOS transcripts is a physiologically important activity of the UPR^{mt}.

Discussion

The pathologies associated with mitochondrial dysfunction are numerous and include neurodegenerative (Rugarli and Langer, 2012) and mitochondrial diseases (Vafai and Mootha, 2012), bacterial infection (Pellegrino et al., 2014), as well as general aging in otherwise healthy individuals (Park and Larsson, 2011). However, the cellular mechanisms and pathways in place to survive mitochondrial stress and ultimately promote recovery are only beginning to be understood. Our data suggest that regenerating or rebuilding defective mitochondria is different and potentially more tightly coordinated than mitochondrial biogenesis in developing healthy cells. The current study provides a unique and unexpected role for ATFS-1 during mitochondrial stress and UPR^{mt} activation. In addition to mediating the transcriptional induction of a mitochondrial protective response that increases the organelle's proteostasis capacity, ATFS-1 restricted expression of mitochondrial and nuclear-encoded OXPHOS transcripts, ultimately promoting respiratory recovery from mitochondrial stress, suggesting that ATFS-1 coordinates the rate of OXPHOS complex biogenesis to match the complex assembly capacity of the defected organelles.

Our studies evolved from a ChIP-seq experiment to determine where in the genome ATFS-1 bound during stress to complement our previous studies that identified a number of *atfs-1*-dependent genes induced during mitochondrial stress including mitochondrial proteostasis (Nargund et al., 2012). ChIP-seq indicated that ATFS-1 bound directly to the promoters of many of these genes during mitochondrial stress suggesting that induction is mediated by direct ATFS-1 binding. Importantly, the ChIP-seq analysis identified many additional genes potentially regulated by ATFS-1 including every glycolysis gene, as well as multiple TCA cycle and OXPHOS genes suggesting that during the UPR^{mt}, ATFS-1 plays a role in metabolic regulation or adaptation to promote recovery from mitochondrial dysfunction. As described, we found that ATFS-1 was a positive regulator of glycolysis gene transcription during mitochondrial stress suggesting the UPR^{mt} promotes an alternative form of ATP production (Nargund et al., 2012). Unlike glycolysis genes, TCA cycle and OXPHOS genes were further increased in worms lacking *atfs-1* indicating *atfs-1* is a negative regulator of TCA cycle and OXPHOS mRNA accumulation. *atfs-1*-deletion also resulted in a further increase of mtDNA-encoded transcripts indicating that *atfs-1* also negatively regulates mtDNA transcript accumulation.

The identification of a nuclear transcription factor that also interacts with mtDNA is not unprecedented (Szczepanek et al., 2012). A recent analysis of multiple mammalian ChIP-seq datasets suggests that a number of nuclear transcription factors also bind mtDNA although the potential regulatory roles of each were not examined (Marinov et al., 2014). Additionally, the estrogen receptors alpha and beta have been found to accumulate in the nucleus and mitochondria and promote mitochondrial biogenesis (Chen et al., 2004). However, the role of the mitochondrial-localized estrogen receptor has proved difficult to elucidate (Klinge, 2008). Because ATFS-1 has clearly defined mitochondrial and nuclear localization sequences, we were able to separate the mitochondrial and nuclear activities of ATFS-1 to demonstrate the physiologic relevance of the mitochondrial-localized fraction. Worms expressing ATFS-1 lacking the MTS induce transcription of nuclear-encoded genes similar to wild-type worms during mitochondrial stress, but fail to limit the accumulation of

mtDNA-encoded mRNAs. Interestingly, these worms have OXPHOS complex assembly defects, reduced oxygen consumption and are developmentally impaired indicating a protective role for the mitochondrial fraction of ATFS-1.

During stress, mitochondrial import defects cause ATFS-1 to traffic to the nucleus. A percentage of ATFS-1 also accumulates within mitochondria, binds mtDNA, and limits mtDNA-encoded mRNA accumulation although the mechanism is unclear. Intriguingly, ATFS-1 binds its own promoter, which coincides with increased transcription of an *atfs-1* splice variant lacking a 16 amino acid sequence near the MTS suggesting the splice isoform may preferentially interact with mtDNA or regulate mtDNA-encoded transcripts. Alternatively, mitochondrial stress-dependent processing of ATFS-1 may contribute to its stability within mitochondria. However, inhibition of the Lon protease, which degrades ATFS-1 within mitochondria in the absence of stress, did not impair mtDNA-encoded transcript accumulation (Figures S6A-D). While our data are consistent with ATFS-1 impairing transcription, we cannot rule out effects of ATFS-1 on mitochondrial mRNA turnover.

The discovery that *atfs-1* affects transcript levels of OXPHOS genes encoded by separate genomes provides an interesting perspective on mitochondrial adaptation during mitochondrial dysfunction. Maintaining and ultimately recovering mitochondrial function during mitochondrial stress is likely a complicated process requiring the coordination of multiple signaling pathways and cellular functions. While ATFS-1 antagonizes OXPHOS transcript accumulation during mitochondrial dysfunction, our data indicate that a separate stress induced compensatory pathway is activated to induce OXPHOS gene transcription (for example, Figures 3E, 4F, and 5G; lanes 1 and 2). The identification of this unknown transcription factor and the potential mechanism by which it is antagonized by ATFS-1 is currently under investigation.

What differentiates the positive regulation of mitochondrial chaperone, OXPHOS complex assembly factors, and glycolysis genes and the negative regulation of OXPHOS genes by ATFS-1 is unclear. Negative regulation of some nuclear-encoded OXPHOS genes by ATFS-1 involves direct promoter binding by ATFS-1 (Figure 4), but the promoters of these genes do not contain obvious UPR^{mt}Es suggesting that ATFS-1 when bound as a repressor may have a distinct binding site. As ATFS-1 was the only bZip protein found to be required for the induction of mitochondrial chaperone genes, we hypothesize it functions as a homo-dimer (Haynes et al., 2010). However, bZip proteins can also form hetero-dimers to regulate transcription (Reinke et al., 2013). Because *atfs-1* also negatively regulates OXPHOS transcripts that are not bound by ATFS-1 (Fig S4A-H), we favor a model where ATFS-1 forms a hetero-dimer with the stimulatory transcription factor impairing its activity. Of course, we cannot exclude the potential effects of chromatin structure or markings on OXPHOS transcript regulation by ATFS-1.

In sum, our data suggests that ATFS-1 optimizes OXPHOS complex assembly by at least two mechanisms (Figure 7H). Once activated, ATFS-1 traffics to the nucleus and activates transcription of a number of genes that promote mitochondrial proteostasis and OXPHOS complex assembly. Simultaneously, ATFS-1 coordinately reduces OXPHOS transcript

accumulation from both genomes to match OXPHOS complex biogenesis rates to the protein folding and complex assembly capability of the defective organelles, ultimately promoting efficient respiratory recovery during mitochondrial dysfunction.

Experimental Procedures

Worm strains and plasmids

The reporter strain *hsp-60$_{pr}$::gfp(zcIs9)V*, the *atfs-1 (tm4525)* allele and he *hsp-60$_{pr}$::gfp* plasmid have been described previously (Baker et al., 2012; Nargund et al., 2012; Yoneda et al., 2004). To generate the *hsp-60$_{pr}$*::gfp* plasmid that lacks a UPR^{mt}E, the ATGATGCAA sequence located 533 base pairs upstream of the start codon was mutated to GATATCCAA using standard molecular biology techniques. The *hsp-60$_{pr}$*::gfp* plasmid (5 ng/μl) was co-injected with a *lin-15* rescuing plasmid and pBluescript (65 ng/μl) into *lin-15(n765ts)* worms generating multiple stable extra-chromosomal arrays. The plasmids expressing transgenic ATFS-1 have been described previously (Nargund et al., 2012).

Microscopy

C. elegans were imaged using a Zeiss AxioCam MRm mounted on a Zeiss Imager.Z2 microscope.

ChIP-Sequencing and Bioinformatics

ChIP assays were performed as described (Rechtsteiner et al., 2010). In brief, synchronized worms were raised in liquid under the described conditions and harvested at the L4 stage by sucrose flotation. Cross-linking of DNA and protein was performed by treating the worms with 11% formaldehyde at 4°C for one hour. The worms were then lysed via Teflon homogenizer and sonicated to obtain 500-1000 base pair DNA fragments. ATFS-1 was then immunoprecipitated from 500 μg of lysate using ATFS-1 antibodies (Nargund et al., 2012) and protein A sepharose beads (Invitrogen). The cross-links were reversed by incubation at 65°C for 5 hours. The DNA fragments were then ethanol-precipitated and purified using QiaQuick Spin Columns (Qiagen). The DNA fragments were sequenced using the Hi-Seq Illumina platform. The raw sequence data obtained by sequencing was first clipped for adapter sequences and then mapped to the *C. elegans* genome (ce6 from UC Santa Cruz) using BWA MEM (version 0.7.5). The output SAM files were processed and sorted with the Picard tools and then peaks were determined using MACS version 1.4 with the no-model parameter. Alternatively, the DNA fragments were quantified via qPCR using the promoter specific primers (Table S5).

To support the binding of ATFS-1 to mtDNA, additional analysis was performed to remove sequences that mapped to mtDNA as well as to the nuclear genome. The output mapping files (BAM files) were filtered with SAMtools to remove any read that had a mapping quality less than 10: SAMtools view −b −q 10 input.bam > output.bam.

To identify candidate UPR^{mt}E motifs, several promoter regions that were enriched in the ChIP-seq using anti-ATFS-1 such as *atfs-1, hsp-60, mthsp-70, dnj-10, tim-17, tim-23, ymel-1, drp-1, gpd-2, mff-2, ldh-1, dct-1, F56C11.3, T09F3.2,* and *F25B4.4* were examined

using the MEME motif analysis program (http://meme.sdsc.edu) (Bailey et al., 2009). To identify motifs potentially involved in repressing nuclear-encoded TCA cycle and OXPHOS genes the promoters of the *nuo-3*, *nuo-4*, *nduf-2.2*, *nduf-6*, *nduf-7*, *Y51H1A.3*, *sdha-1*, *cyc-2.1*, *cco-1*, *cco-2*, *atp-2*, *atp-3*, *H28O16.1*, *F58F12.1*, *aco-2*, *cts-1* and *mdh-1* genes enriched in the ATFS-1 ChIP-seq were similarly examined using the MEME motif analysis program.

RNA isolation and quantitative RT-PCR

Total RNA was isolated using the RNA STAT reagent (Tel-Test) and treated with DNAse (Ambion). cDNA was then synthesized from total RNA using the iScript™ cDNA Synthesis Kit (Bio-Rad Laboratories). qPCR was used to determine the expression levels of the indicated genes using iQ™ sybr green supermix and MyiQ™2 Two-Color Real-Time PCR Detection System (Bio-Rad). Gene specific primers are listed in Table S6. Actin was used as a control. Fold changes in gene expression were calculated using the comparative CtΔΔCt method.

Mitochondrial genome quantitation

mtDNA quantitation was measured by qPCR as described (Bratic et al., 2009; Bratic et al., 2010).

Electrophoretic mobility shift assay (EMSA)

GST-ATFS-1 was expressed in *E. coli* (BL21) as described (Nargund et al, 2012). GST-ATFS-1 was affinity purified using GST-spin trap columns (GE Healthcare). The EMSA was performed as described (Sano et al, 2001). 3 μg of purified ATFS-1 was incubated with pre-annealed IRDye700 labeled oligonucleotides (Integrated DNA technologies) composed of the mtDNA non-coding region including the UPR^{mt}E (Table S7). Identical duplexed DNA with a scrambled UPR^{mt}E was used to verify the specificity of the DNA-protein complex. The mixture was then separated on a 4% native polyacrylamide gel and imaged using an Odyssey Infrared Imager (Li-Cor Biosciences). EMSA was performed multiple times.

Oxygen consumption

Oxygen consumption assays were performed as described (Haynes et al., 2010) using a Clark type electrode (Braeckman et al., 2002).

Protein analysis and antibodies

Whole worm lysates as well as cellular fractionation were performed as previously described (Nargund et al., 2012). Antibodies against α-tubulin were purchased from Calbiochem, NDUFS3 (*nuo-2* in *C. elegans*, complex I) antibodies from MitoSciences, ATP5A (H28O16.1 in *C. elegans*, complex V) and COX1 (Anti-MTCO1) from Abcam. Immunoblots were visualized using an Odyssey Infrared Imager (Li-Cor Biosciences). All western blot experiments were performed multiple times.

Blue Native PAGE

Blue native PAGE was performed essentially as described (Pujol et al., 2013; van den Ecker et al., 2010). Briefly, wild-type and *atfs-1(tm4525)* worms were synchronized by bleaching, raised on either control or *spg-7*(RNAi) and harvested at the L4 stage. Worm lysates were obtained using a Teflon homogenizer. 50 μg of lysate were solubilized using 1% digitonin and subsequently, 25 μg of total protein was separated on 3-12% native gel (Native-PAGE Novex 3-12% gel from Invitrogen) using Xcell SureLock Mini Cell (Invitrogen). Western blots were performed rather than the standard coomassie staining as it was difficult to obtain high enough quantities of purified mitochondria from the *spg-7*(RNAi) treated *atfs-1(tm4525)* worms. For the western blots, the antibodies described above were used along with secondary antibodies conjugated to horseradish peroxidase.

Supplementary Material

Refer to Web version on PubMed Central for supplementary material.

Acknowledgments

We thank Nicholas Socci, Aleksandra Trifunovic, Susan Strome and Yi-Fan Lin for advice, the National BioResource Project and the Caenorhabditis Genetics Center for worm strains and the Genomics and Bioinformatics Facilities at Memorial Sloan Kettering Cancer Center. This work was supported by the Alfred W. Bressler Scholar Fund, the Ellison Medical Foundation, and NIH grants R01AG040061 (CMH) and NRSA F32GM102974 (AMN).

References

Bailey TL, Boden M, Buske FA, Frith M, Grant CE, Clementi L, Ren J, Li WW, Noble WS. MEME SUITE: tools for motif discovery and searching. Nucleic acids research. 2009; 37:W202–208. [PubMed: 19458158]

Baker BM, Nargund AM, Sun T, Haynes CM. Protective coupling of mitochondrial function and protein synthesis via the eIF2alpha kinase GCN-2. PLoS genetics. 2012; 8:e1002760. [PubMed: 22719267]

Bestwick ML, Shadel GS. Accessorizing the human mitochondrial transcription machinery. Trends in biochemical sciences. 2013

Braeckman BP, Houthoofd K, Vanfleteren JR. Assessing metabolic activity in aging Caenorhabditis elegans: concepts and controversies. Aging cell. 2002; 1:82–88. discussion 102-103. [PubMed: 12882336]

Bratic I, Hench J, Henriksson J, Antebi A, Burglin TR, Trifunovic A. Mitochondrial DNA level, but not active replicase, is essential for Caenorhabditis elegans development. Nucleic acids research. 2009; 37:1817–1828. [PubMed: 19181702]

Bratic I, Hench J, Trifunovic A. Caenorhabditis elegans as a model system for mtDNA replication defects. Methods. 2010; 51:437–443. [PubMed: 20230897]

Buske FA, Boden M, Bauer DC, Bailey TL. Assigning roles to DNA regulatory motifs using comparative genomics. Bioinformatics. 2010; 26:860–866. [PubMed: 20147307]

Chen JQ, Eshete M, Alworth WL, Yager JD. Binding of MCF-7 cell mitochondrial proteins and recombinant human estrogen receptors alpha and beta to human mitochondrial DNA estrogen response elements. Journal of cellular biochemistry. 2004; 93:358–373. [PubMed: 15368362]

Dennis G Jr, Sherman BT, Hosack DA, Yang J, Gao W, Lane HC, Lempicki RA. DAVID: Database for Annotation, Visualization, and Integrated Discovery. Genome biology. 2003; 4:3.

Falkenberg M, Larsson NG, Gustafsson CM. DNA replication and transcription in mammalian mitochondria. Annual review of biochemistry. 2007; 76:679–699.

Ghezzi D, Zeviani M. Assembly factors of human mitochondrial respiratory chain complexes: physiology and pathophysiology. Advances in experimental medicine and biology. 2012; 748:65–106. [PubMed: 22729855]

Haynes CM, Yang Y, Blais SP, Neubert TA, Ron D. The matrix peptide exporter HAF-1 signals a mitochondrial UPR by activating the transcription factor ZC376.7 in C. elegans. Molecular cell. 2010; 37:529–540. [PubMed: 20188671]

Houtkooper RH, Mouchiroud L, Ryu D, Moullan N, Katsyuba E, Knott G, Williams RW, Auwerx J. Mitonuclear protein imbalance as a conserved longevity mechanism. Nature. 2013; 497:451–457. [PubMed: 23698443]

Klinge CM. Estrogenic control of mitochondrial function and biogenesis. Journal of cellular biochemistry. 2008; 105:1342–1351. [PubMed: 18846505]

Leonhard K, Guiard B, Pellecchia G, Tzagoloff A, Neupert W, Langer T. Membrane protein degradation by AAA proteases in mitochondria: extraction of substrates from either membrane surface. Molecular cell. 2000; 5:629–638. [PubMed: 10882099]

Mick DU, Fox TD, Rehling P. Inventory control: cytochrome c oxidase assembly regulates mitochondrial translation. Nature reviews Molecular cell biology. 2011; 12:14–20.

Mimaki M, Wang X, McKenzie M, Thorburn DR, Ryan MT. Understanding mitochondrial complex I assembly in health and disease. Biochimica et biophysica acta. 2012; 1817:851–862. [PubMed: 21924235]

Nargund AM, Pellegrino MW, Fiorese CJ, Baker BM, Haynes CM. Mitochondrial import efficiency of ATFS-1 regulates mitochondrial UPR activation. Science. 2012; 337:587–590. [PubMed: 22700657]

Nolden M, Ehses S, Koppen M, Bernacchia A, Rugarli EI, Langer T. The m-AAA protease defective in hereditary spastic paraplegia controls ribosome assembly in mitochondria. Cell. 2005; 123:277–289. [PubMed: 16239145]

Oliveira RP, Porter Abate J, Dilks K, Landis J, Ashraf J, Murphy CT, Blackwell TK. Condition-adapted stress and longevity gene regulation by Caenorhabditis elegans SKN-1/Nrf. Aging cell. 2009; 8:524–541. [PubMed: 19575768]

Pagliarini DJ, Calvo SE, Chang B, Sheth SA, Vafai SB, Ong SE, Walford GA, Sugiana C, Boneh A, Chen WK, et al. A mitochondrial protein compendium elucidates complex I disease biology. Cell. 2008; 134:112–123. [PubMed: 18614015]

Park CB, Larsson NG. Mitochondrial DNA mutations in disease and aging. The Journal of cell biology. 2011; 193:809–818. [PubMed: 21606204]

Pellegrino MW, Nargund AM, Kirienko NV, Gillis R, Fiorese CJ, Haynes CM. Mitochondrial UPR-regulated innate immunity provides resistance to pathogen infection. Nature. 2014

Pujol C, Bratic-Hench I, Sumakovic M, Hench J, Mourier A, Baumann L, Pavlenko V, Trifunovic A. Succinate dehydrogenase upregulation destabilize complex I and limits the lifespan of gas-1 mutant. PloS one. 2013; 8:e59493. [PubMed: 23555681]

Rechtsteiner A, Ercan S, Takasaki T, Phippen TM, Egelhofer TA, Wang W, Kimura H, Lieb JD, Strome S. The histone H3K36 methyltransferase MES-4 acts epigenetically to transmit the memory of germline gene expression to progeny. PLoS genetics. 2010; 6:e1001091. [PubMed: 20824077]

Reinke AW, Baek J, Ashenberg O, Keating AE. Networks of bZIP protein-protein interactions diversified over a billion years of evolution. Science. 2013; 340:730–734. [PubMed: 23661758]

Rugarli EI, Langer T. Mitochondrial quality control: a matter of life and death for neurons. The EMBO journal. 2012; 31:1336–1349. [PubMed: 22354038]

Sano M, Ohyama A, Takase K, Yamamoto M, Machida M. Electrophoretic mobility shift scanning using an automated infrared DNA sequencer. BioTechniques. 2001; 31:1056–1058. 1060, 1062. [PubMed: 11730013]

Scarpulla RC, Vega RB, Kelly DP. Transcriptional integration of mitochondrial biogenesis. Trends in endocrinology and metabolism: TEM. 2012; 23:459–466. [PubMed: 22817841]

Schreiber SN, Emter R, Hock MB, Knutti D, Cardenas J, Podvinec M, Oakeley EJ, Kralli A. The estrogen-related receptor alpha (ERRalpha) functions in PPARgamma coactivator 1alpha

(PGC-1alpha)-induced mitochondrial biogenesis. Proceedings of the National Academy of Sciences of the United States of America. 2004; 101:6472–6477. [PubMed: 15087503]

Szczepanek K, Lesnefsky EJ, Larner AC. Multi-tasking: nuclear transcription factors with novel roles in the mitochondria. Trends in cell biology. 2012; 22:429–437. [PubMed: 22705015]

Vafai SB, Mootha VK. Mitochondrial disorders as windows into an ancient organelle. Nature. 2012; 491:374–383. [PubMed: 23151580]

van den Ecker D, van den Brand MA, Bossinger O, Mayatepek E, Nijtmans LG, Distelmaier F. Blue native electrophoresis to study mitochondrial complex I in C. elegans. Analytical biochemistry. 2010; 407:287–289. [PubMed: 20705045]

Wu Z, Puigserver P, Andersson U, Zhang C, Adelmant G, Mootha V, Troy A, Cinti S, Lowell B, Scarpulla RC, et al. Mechanisms controlling mitochondrial biogenesis and respiration through the thermogenic coactivator PGC-1. Cell. 1999; 98:115–124. [PubMed: 10412986]

Yoneda T, Benedetti C, Urano F, Clark SG, Harding HP, Ron D. Compartment-specific perturbation of protein handling activates genes encoding mitochondrial chaperones. Journal of cell science. 2004; 117:4055–4066. [PubMed: 15280428]

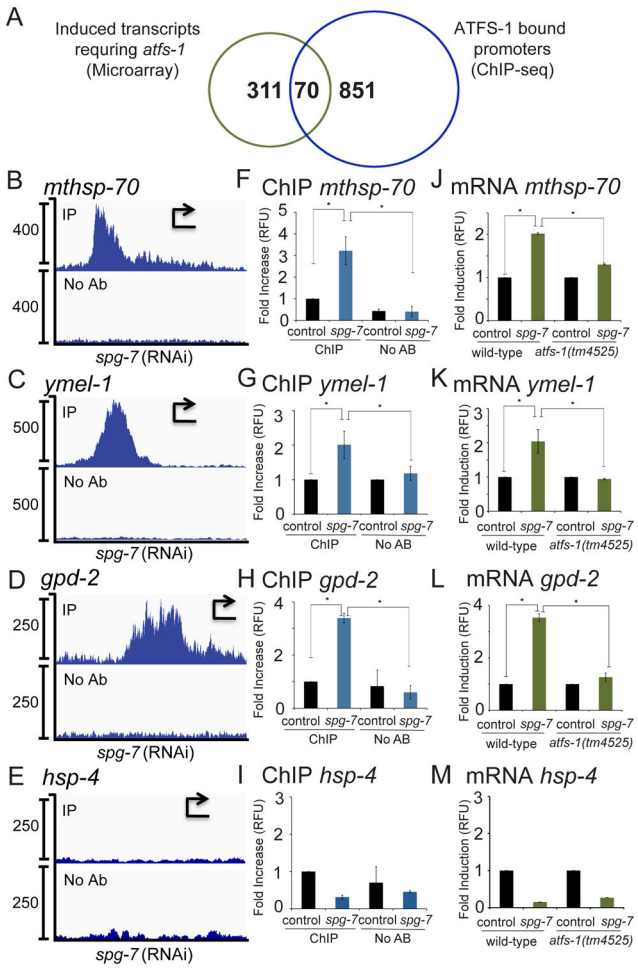

Fig. 1. ATFS-1 interacts with the promoters of mitochondrial protective genes induced during mitochondrial stress

A. Venn diagram illustrating the genes induced in an *atfs-1*-dependent manner during mitochondrial stress (Nargund et al., 2012), and the gene promoters that ATFS-1 bound during mitochondrial stress identified by ChIP-seq, and the overlap.

B-E. ChIP-seq profiles of the *mthsp-70*, *ymel-1*, *gpd-2* and *hsp-4* promoters in wild-type worms raised on *spg-7*(RNAi), using ATFS-1 antibody (upper panel) or no antibody (lower panel). The y-axis is the number of sequence reads and the x-axis is approximately 2.5 kilobases with the start codon marked with an arrowhead.

F-I. ChIP of the promoters in Figures 1B-E in the presence or absence of ATFS-1 antibody from wild-type worms raised on control or *spg-7*(RNAi) as measured by qPCR (N = 3, ± SD, p* (student t-test) < 0.05).

J-M. Expression levels of *mthsp-70*, *ymel-1*, *gpd-2* and *hsp-4* mRNA in wild-type or *atfs-1(tm4525)* worms raised on control or *spg-7*(RNAi) determined by qRT-PCR (N = 3, ± SD, p* (student t-test) < 0.05) (right panels).

See also Figure S1 and Tables S1 and S2.

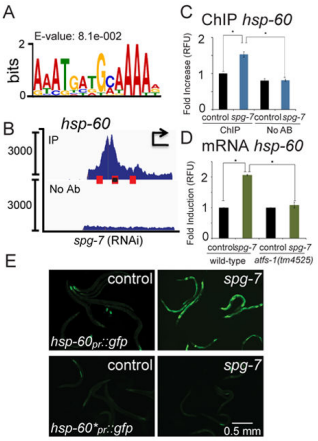

Fig. 2. ATFS-1 binds to the UPR^{mt}E and induces mitochondrial chaperone transcription during stress

A. The UPR^{mt}E consensus sequence.

B. ChIP-seq profile of the *hsp-60* promoter in wild-type worms raised on *spg-7*(RNAi) using ATFS-1 antibody or no antibody. The three UPR^{mt}Es within the promoter are marked with red boxes, and the element mutated in Figure 2E is marked with a black dot. The y-axis is the number of sequence reads and the x-axis is approximately 2.5 kilobases with the start codon marked with an arrowhead. Of note, the majority of the reads come from the multi-copy *hsp-60$_{pr}$::gfp* transgene likely accounting for the high number of reads and the sharp profile borders.

C. ChIP of the *hsp-60* promoter in the presence or absence of ATFS-1 antibody from wild-type worms raised on control or *spg-7*(RNAi) as measured by qPCR (N = 3, ± SD, p* (student t-test) < 0.05).

D. Expression levels of *hsp-60* mRNA in wild-type or *atfs-1(tm4525)* worms raised on control or *spg-7*(RNAi) determined by qRT-PCR (N = 3, ± SD, p* (student t-test) < 0.05).

E. Photomicrographs of *hsp-60$_{pr}$::gfp* (top panels) or *hsp-60$_{pr}$::gfp* lacking a UPR^{mt}E (*) (bottom panels) transgenic worms raised on control or *spg-7*(RNAi). Scale bar, 0.5 mm. See also Figure S2.

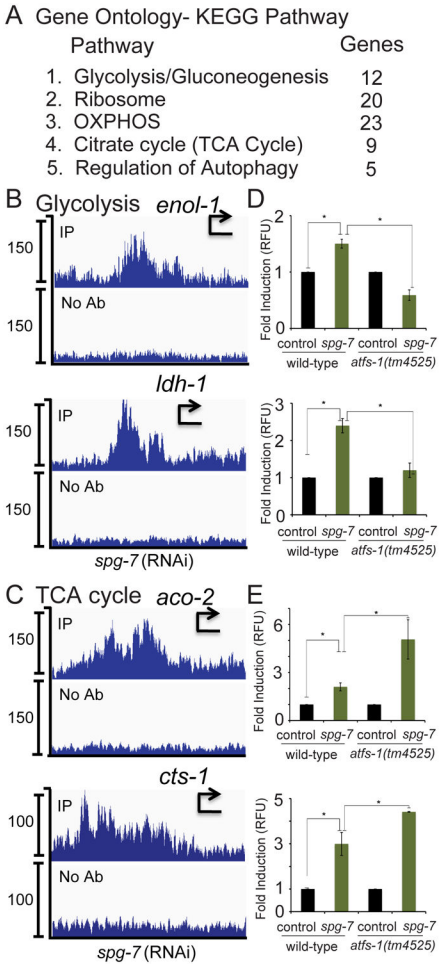

Fig. 3. ATFS-1 interacts with multiple metabolic gene promoters

A. Gene ontology-KEGG Pathway analysis of the genes obtained by ATFS-1 ChIP-seq indicating the five most enriched pathways.

B-C. ChIP-seq profiles of representative genes in the glycolysis (B) and TCA cycle (C) pathways of wild-type worms raised on *spg-7*(RNAi), using ATFS-1 antibody or no antibody. The y-axis is the number of sequence reads and the x-axis is approximately 2.5 kilobases with the start codon marked with an arrowhead.

D-E. Expression levels of the glycolysis transcripts (D) *enol-1* and *ldh-1*, and the TCA cycle transcripts (E) *aco-2* and *cts-1* in wild-type or *atfs-1(tm4525)* worms raised on control or *spg-7*(RNAi) determined by qRT-PCR (N = 3, ± SD, p* (student t-test) < 0.05).

See also Figure S3 and Table S3.

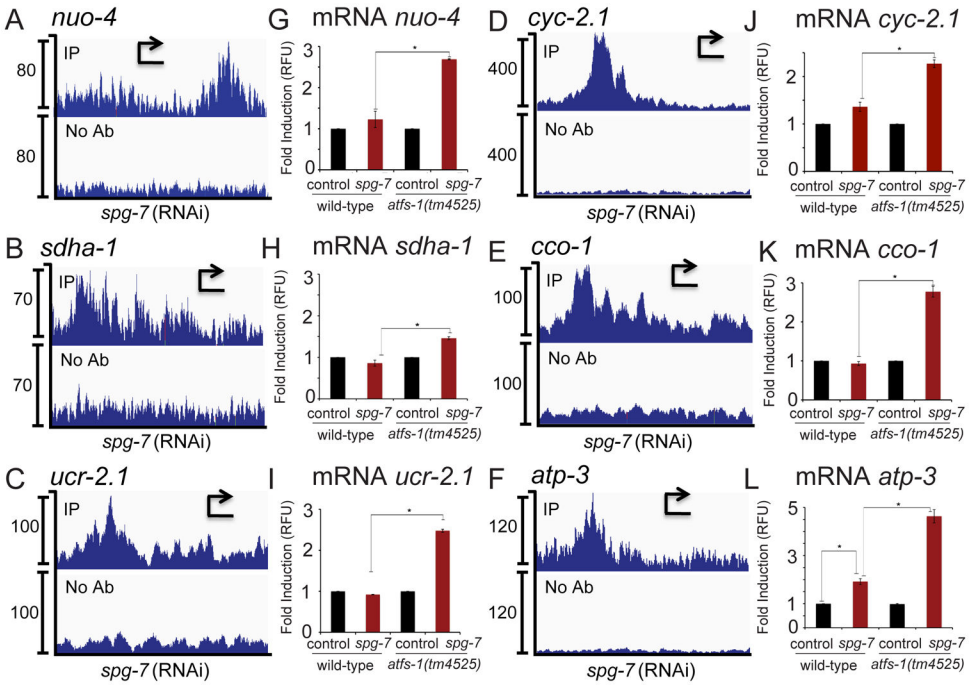

Fig. 4. ATFS-1 limits the accumulation of nuclear-encoded OXPHOS transcripts

A-F. ChIP-seq profiles of representative OXPHOS genes *nuo-4*, *sdha-1*, ucr-*2.1*, *cyc-2.1*, *cco-1*, and *atp-3* of wild-type worms raised on *spg-7*(RNAi), using ATFS-1 antibody or no antibody. The y-axis is the number of sequence reads and the x-axis is approximately 2.5 kilobases with the start codon marked with an arrowhead.

G-L. Expression levels of *nuo-4*, *sdha-1*, ucr-*2.1*, *cyc-2.1*, *cco-1*, and *atp-3* mRNA in wild-type or *atfs-1(tm4525)* worms raised on control or *spg-7*(RNAi) determined by qRT-PCR (N = 3, ± SD, p* (student t-test) < 0.05) (right panels).

See also Figure S4 and Table S4.

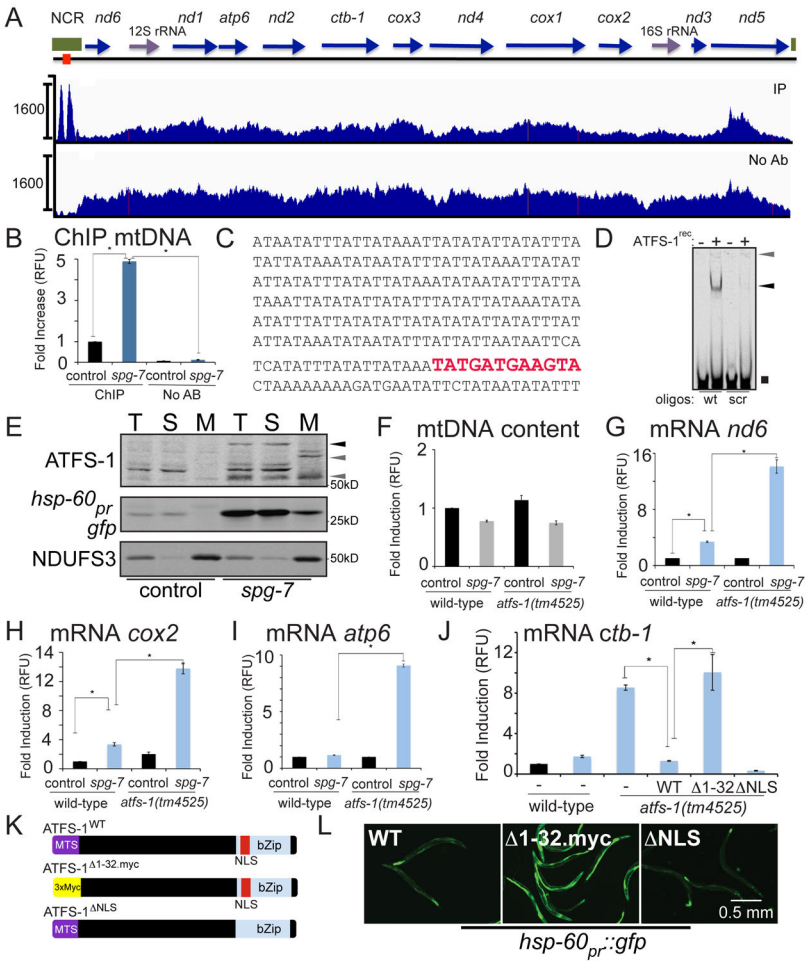

Fig. 5. ATFS-1 limits mtDNA-encoded transcript accumulation and directly binds to the non-coding region of mtDNA

A. ChIP-seq profiles of the entire mitochondrial genome (mtDNA) of wild-type worms raised on *spg-7*(RNAi), using ATFS-1 antibody or no antibody. The y-axis is the number of sequence reads and the x-axis is the 13,794 nucleotide mitochondrial genome. The protein coding genes are marked with blue arrows, the rRNA genes with purple arrows, the non-coding region in green, and the putative UPR^{mt}E is marked with a red box.

B. ChIP of the mtDNA non-coding region in the presence or absence of ATFS-1 antibody from wild-type worms raised on control or *spg-7*(RNAi) as measured by qPCR (N = 3, ± SD, p* (student t-test) < 0.05).

C. mtDNA non-coding region sequence with the putative UPR^{mt}E in red.

D. EMSA using recombinant ATFS-1 and wild-type D-loop oligonucleotides or D-loop oligonucleotides with the 9 base pair UPR^{mt}E scrambled. Unbound oligos (black square), ATFS-1-DNA complex (black arrow) and the loading well (gray arrow) are indicated.

E. Immunoblots of lysates from worms raised on control or *spg-7*(RNAi) following fractionation into total lysate (T), postmitochondrial supernatant (S) and mitochondrial pellet (M) (Nargund et al., 2012). Endogenous NDUFS3 serves as a mitochondrial marker and *hsp-60$_{pr}$::gfp* as a stress-induced cytosolic marker. Full-length (black arrow) and the mitochondrial forms (gray arrows) of ATFS-1 are indicated.

F. Relative mtDNA copy number in wild-type and *atfs-1(tm4525)* worms raised on control or *spg-7*(RNAi) as determined by qPCR (N = 3, ± SD, p* (student t-test) < 0.05).

G-I. Expression levels of the mtDNA-encoded mRNAs *nd6*, *cox2* and *atp6* in wild-type or *atfs-1(tm4525)* worms raised on control or *spg-7*(RNAi) determined by qRT-PCR (N = 3, ± SD, p* (student t-test) < 0.05).

J. Expression level of the mtDNA-encoded *ctb-1* mRNA in wild-type or *atfs-1(tm4525)* worms expressing no transgenes (-) or transgenic wild-type ATFS-1, ATFS-$1^{\Delta 1\text{-}32.myc}$ or ATFS-$1^{\Delta NLS}$ raised on control or *spg-7*(RNAi) determined by qRT-PCR (N = 3, ± SD, p* (student t-test) < 0.05).

K. Schematics of wild-type ATFS-1, ATFS-1 with an impaired mitochondrial targeting sequence (MTS) (ATFS-$1^{\Delta 1\text{-}32.myc}$), and ATFS-1 with a mutated nuclear localization sequence (NLS) (ATFS-$1^{\Delta NLS}$).

L. Fluorescent photomicrographs of *atfs-1(tm4525);hsp-60*$_{pr}$*::gfp* worms expressing transgenic ATFS-1, ATFS-$1^{\Delta 1\text{-}32.myc}$, or ATFS-$1^{\Delta NLS}$ raised at 20°C. Scale bar, 0.5 mm. See also Figure S5.

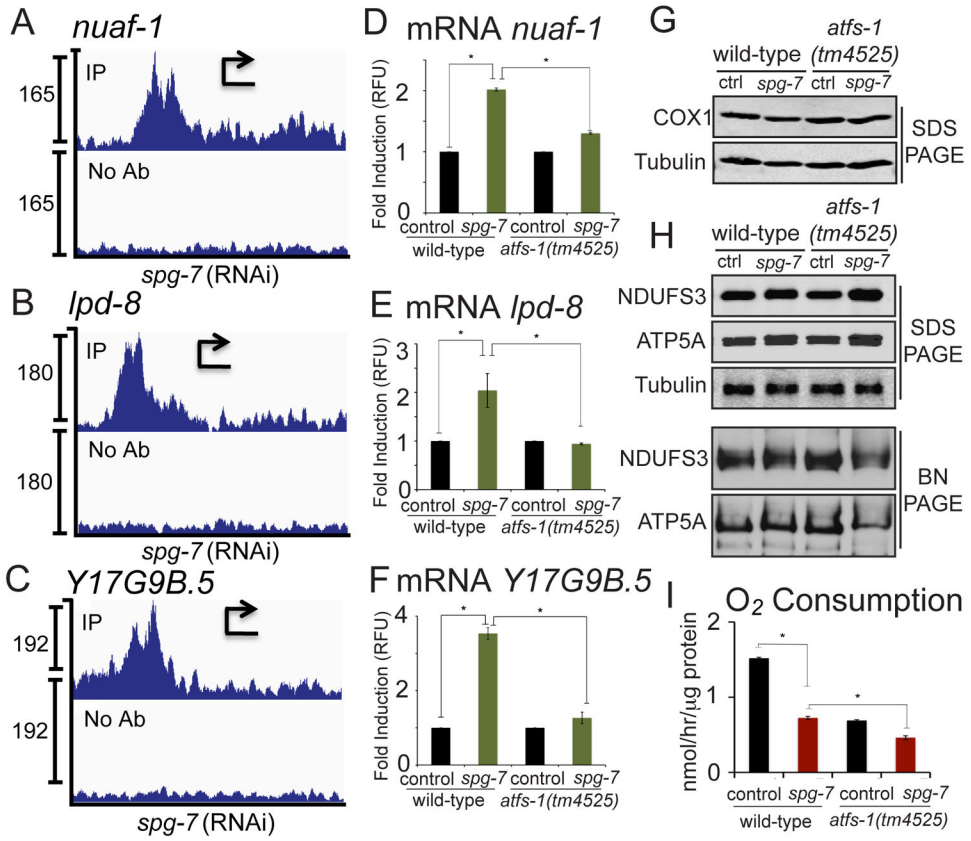

Fig. 6. ATFS-1 promotes OXPHOS complex assembly during mitochondrial dysfunction

A-C. ChIP-seq profiles of *nuaf-1*, *lpd-8*, and *Y17G9B.5* of wild-type worms raised on *spg-7*(RNAi), using ATFS-1 antibody or no antibody. The y-axis is the number of sequence reads and the x-axis is approximately 2.5 kilobases with the start codon marked with an arrowhead.

D-F. Expression levels of *nuaf-1*, *lpd-8*, and *Y17G9B.5* mRNA in wild-type or *atfs-1(tm4525)* worms raised on control or *spg-7*(RNAi) determined by qRT-PCR (N = 3, ± SD, p* (student t-test) < 0.05) (right panels).

G. SDS-PAGE immunoblots of extracts from wild-type and *atfs-1(tm4525)* worms raised on control or *spg*-7(RNAi). COX1 is a component of the cytochrome c oxidase complex (IV) and tubulin was used as a loading control.

H. SDS-PAGE immunoblots of extracts from wild-type and *atfs-1(tm4525)* worms raised on control or *spg*-7(RNAi) (upper three panels). The lower two panels are blue-native PAGE immunoblots of the same extracts. NDUFS3 is a component of the NADH ubiquinone oxidoreductase complex, ATP5A is an ATP synthase component and tubulin was used as a loading control.

I. Oxygen consumption in wild-type or *atfs-1(tm4525)* worms raised on control or *spg-7*(RNAi) (N = 3, ± SD, p* (student t-test) < 0.05).

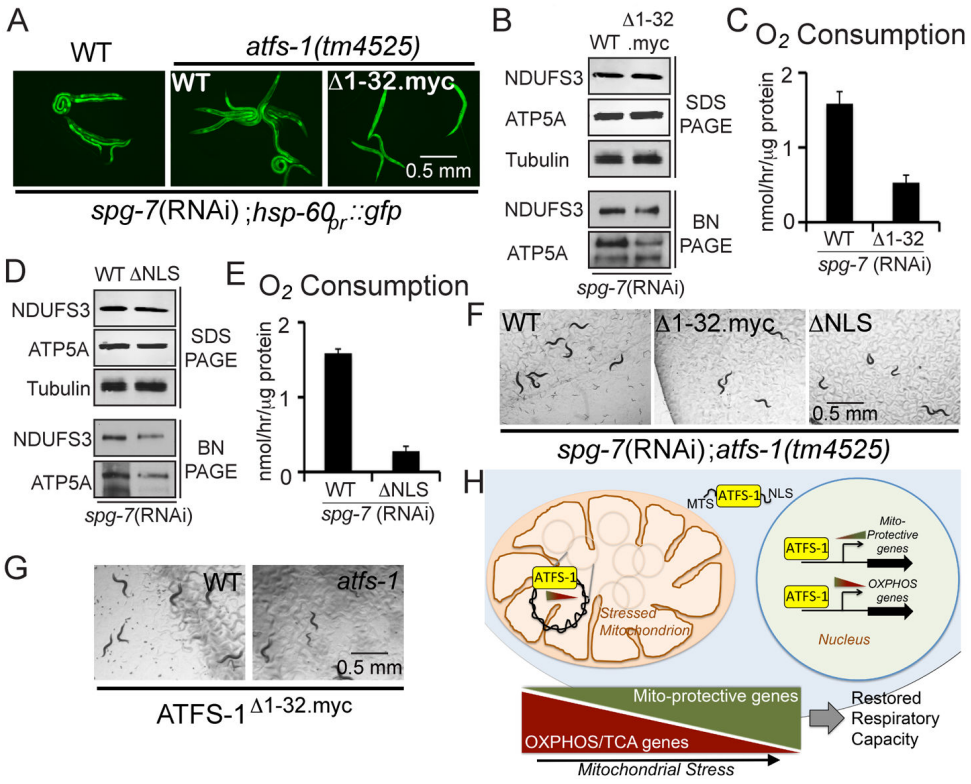

Fig. 7. Mitochondrial and nuclear accumulation of ATFS-1 promotes respiration and development during mitochondrial dysfunction

A. Photomicrographs of wild-type *hsp-60*$_{pr}$*::gfp* and *afts-1(tm4525);hsp-60*$_{pr}$*::gfp* worms expressing transgenic ATFS-1, or ATFS-1$^{\Delta 1\text{-}32myc}$ raised on *spg-7*(RNAi). Scale bar, 0.5 mm.

B. SDS-PAGE immunoblots of extracts from *atfs-1(tm4525)* worms expressing transgenic ATFS-1, or ATFS-1$^{\Delta 1\text{-}32myc}$ raised on *spg-7*(RNAi) (upper three panels). The lower two panels are blue-native PAGE immunoblots of the same extracts.

C. Oxygen consumption in *atfs-1(tm4525)* worms expressing transgenic ATFS-1 or ATFS-1$^{\Delta 1\text{-}32myc}$ raised on *spg-7*(RNAi) (N = 3, ± SD, p* (student t-test) < 0.05).

D. SDS-PAGE immunoblots of extracts from *atfs-1 (tm4525)* worms expressing transgenic ATFS-1 or ATFS-1$^{\Delta NLS}$ raised on *spg-7*(RNAi) (upper three panels). The lower two panels are blue-native PAGE immunoblots of the same extracts.

E. Oxygen consumption in *atfs-1(tm4525)* worms expressing transgenic ATFS-1 or ATFS-1$^{\Delta NLS}$ raised on *spg-7*(RNAi) (N = 3, ± SD, p* (student t-test) < 0.05).

F. Representative photomicrographs of synchronized *afts-1(tm4525);hsp-60*$_{pr}$*::gfp* worms expressing transgenic ATFS-1, ATFS-1$^{\Delta 1\text{-}32myc}$ or ATFS-1$^{\Delta NLS}$ allowed to develop for 72 hours on *spg-7*(RNAi). Note the increased progeny in the ATFS-1^{WT} panel relative to the ATFS-1$^{\Delta 1\text{-}32myc}$ and ATFS-1$^{\Delta NLS}$ panels. Scale bar, 0.5 mm.

G. Representative photomicrographs of synchronized wild-type or *afts-1(tm4525)* worms expressing transgenic ATFS-1 $^{\Delta 1\text{-}32myc}$. Scale bar, 0.5 mm.

H. Signaling model depicting ATFS-1's function during mitochondrial stress.

See also Figure S6.